

# DEUTSCHES ELEKTRONEN-SYNCHROTRON DESY

DESY 74/22  
May 1974



Momentum Distribution of Bound State Protons Derived  
from Quasi-Free Electron Scattering on  $^{12}\text{C}$

by



M. Köbberling, J. Moritz, K. H. Schmidt, D. Wegener and J. Zeller  
*Institut für Experimentelle Kernphysik der Universität (TH)  
und des Kernforschungszentrums Karlsruhe*

J. K. Bienlein, J. Bleckwenn, H. Dinter  
*Deutsches Elektronen-Synchrotron DESY, Hamburg*

F. H. Heimlich  
*Physikalisches Institut der Universität Freiburg/Breisgau*

2 HAMBURG 52 . NOTKESTIEG 1

To be sure that your preprints are promptly included in the  
HIGH ENERGY PHYSICS INDEX ,  
send them to the following address ( if possible by air mail ) :

DESY  
Bibliothek  
2 Hamburg 52  
Notkestieg 1  
Germany

MOMENTUM DISTRIBUTION OF BOUND STATE PROTONS DERIVED  
FROM QUASI-FREE ELECTRON SCATTERING ON  $^{12}\text{C}$

M. Köbberling, J. Moritz, K.H. Schmidt, D. Wegener  
and D. Zeller

Institut für Experimentelle Kernphysik der Universität (TH)  
und des Kernforschungszentrums Karlsruhe

J.K. Bienlein, J. Bleckwenn, H. Dinter  
Deutsches Elektronen-Synchrotron DESY, Hamburg

F.H. Heimlich

Physikalisches Institut der Universität Freiburg/Breisgau

ABSTRACT

Quasi-elastic electron scattering from  $^{12}\text{C}$  in the range of the four momentum transfer  $5 \text{ fm}^{-2} \leq q^2 \leq 11 \text{ fm}^{-2}$  was measured. The momentum distribution of the bound state protons derived from this experiment shows a large tail of high momenta. Nuclear wave functions including short range nucleon-nucleon correlations with a parameter  $q_c = 300 \text{ MeV}/c$  give a better fit to the data than pure shell model wave functions.

Several authors have pointed out that quasi-elastic electron scattering is a powerful tool to investigate the properties of single nucleons in a nucleus and in particular, the single particle momentum distribution<sup>1</sup>.

Until now the experimental data<sup>2,3</sup> have covered a range of the momentum of the bound state nucleon up to about  $1 \text{ fm}^{-1}$ . With electrons of 2.7 GeV primary energy we were able to measure the momentum distribution up to momenta of about  $2 \text{ fm}^{-1}$ .

In the present experiment<sup>4</sup> we determined the threefold differential cross section for quasi-elastic scattering of electrons from  $^{12}\text{C}$  in the range of the four momentum transfer of  $5 \text{ fm}^{-2} \leq q^2 \leq 11 \text{ fm}^{-2}$ .

The slowly ejected electron beam of 2.5 and 2.7 GeV of the DESY synchrotron was focussed on a 2mm thick carbon target. The momenta and the angles of the scattered electrons were measured with a spectrometer which consisted of a magnet with a homogeneous field, four wire spark chambers with ferrit core read-out, and a set of scintillation counters, including a shower counter<sup>5</sup>. This spectrometer has the advantage of having a momentum acceptance of  $\pm 20\%$  which allows the measurement of the electron spectra of the whole quasi-elastic peak with one spectrometer setting. The momenta of the scattered electrons were measured with an accuracy of  $\Delta p/p = \pm 0.6\%$  and the scattering angle with an accuracy of  $\pm 0.1 \text{ mrad}$ .

In order to detect the recoil protons a scintillation counter hodoscope was mounted on a platform pivoting horizontally around the target. This hodoscope consisted of 12 horizontal and 12 vertical 1cm thick scintillation counters which form a matrix of 144 elements subtending a solid angle of

$31^\circ \times 31^\circ$  around the direction of the virtual photon. With this large solid angle the apparatus accepted events with momenta of the bound state protons up to  $2 \text{ fm}^{-1}$  before the scattering process. Four additional 5cm thick scintillation counters behind the matrix were installed for better pulse height analysis. Each of the 28 scintillation counters of the hodoscope was connected to an amplitude to digital converter. All experimental data were stored on-line by a CDC 1700 computer, which also monitored continuously the performance of the apparatus during the run<sup>6</sup>.

We analyzed only these events where one counter in each plane had fired in coincidence with the electron spectrometer. This gives an angular resolution for the detection of the recoil protons of  $\pm 1.3^\circ$ .

We compared the set of pulse heights of each particle in the three counter planes with calibration measurements from elastic electron-proton scattering. Thus we were able to separate between protons, pions, and other background particles in the counter hodoscope by pulse height analysis. Moreover, these measurements allowed a determination of systematic errors.

Fig. 1 shows the angular distribution of the recoil protons for two different energies of the scattered electrons. The errors of the experimental points are due to statistics only.

From the momentum and the direction of the scattered electron and the direction of the recoil proton we computed the momentum  $\vec{p}_R$  of the residual nucleus

$$\vec{p}_R = \vec{q} - \vec{p}_4$$

for each event.  $\vec{q}$  is the momentum of the virtual photon and  $\vec{p}_4$  is the momentum of the recoil proton with

$$|\vec{p}_4| = \frac{|\vec{q}|}{A} \cos \phi_{q4} + \sqrt{\frac{|\vec{q}|^2}{A^2} \cos^2 \phi_{q4} - \frac{q^2}{A} + \frac{2M_p(A-1)}{A}(E_1 + \epsilon - E_3)}$$

$A=12$ : atomic number of the  $^{12}\text{C}$ -nucleus

$\phi_{q4}$ : angle between the virtual photon and the recoil proton

$M_p$ : mass of the proton

$E_1$ : energy of the primary electron

$E_3$ : energy of the scattered electron

$\epsilon$  is the separation energy of the bound state proton. Since we did not measure the energy of the recoil proton we were not able to separate protons ejected from different nuclear shells. Therefore we have chosen a mean separation energy of  $\epsilon = 25$  MeV.

In this experiment the energies of the recoil protons were high enough to neglect the real part of the optical potential for the outgoing protons<sup>7</sup>. Therefore the data of this experiment can be considered as an incoherent sum of quasi-elastic electron scattering on protons from the s- and p-shell of the  $^{12}\text{C}$ -nucleus. Applying the impulse approximation means that  $q_p$  is identical with the momentum  $p_2$  of the bound state proton before the scattering process.

In table 1 the momentum distributions of the bound state protons in carbon are listed for the three kinematic parameters of this experiment. Only the statistical errors are given in this table. The overall systematic errors are of the order of  $\pm 3.5\%$ . The data of the three measurements agree perfect for

$$|p_2| < 0.92 \text{ fm}^{-1} .$$

It is convenient to compare the experimental data with nuclear wave functions describing the low energy data. Therefore, we used a Woods-Saxon shell model wave function with parameters determined from the separation energies and from fits to elastic electron scattering<sup>8</sup>. To take into account the short range effects in the nucleus we utilized shell model wave functions which were modified by short range nucleon-nucleon correlations. These correlations were introduced into the independent particle model by means of the Jastrow method<sup>9</sup> and parametrized by a definite momentum  $q_c$  which is exchanged between two otherwise independently moving nucleons<sup>10</sup>.

To fit the angular distribution of the recoil protons, we have chosen the representation of Devanathan<sup>11</sup> for the three-fold differential cross section, which has the advantage that the momentum distribution of the bound state nucleons can be factorized. The full drawn curve in fig. 1 is the result of this calculation. Radiative corrections are included according to the method of Mo and Tsai<sup>12</sup>. In case of large energy loss of the scattered electron, the result of the calculation and the experimental points do not fit too well. This is due to the fact that the high momentum tail of the momentum distribution of the bound state protons, as given by the shell model including correlations, has to be increased to fit our data.

Fig. 2 shows that the wave function with a correlation parameter  $q_c = 300$  MeV/c is in better agreement with our momentum distribution than the pure shell model curve. But in the high momentum range even the curve with correlations is too low. This is in agreement with results obtained from quasi-elastic electron scattering from  ${}^6\text{Li}$  in the same kinematic region<sup>13</sup>.

It is remarkable that the correlation parameter  $q_c = 300 \text{ MeV}/c$  has also been derived in the analysis of quite different experiments, e.g. the absorption of photons and pions by nuclei <sup>14</sup> which are characterized respectively by an absorbed particle on the light cone and in the time like region, while in the present experiment a space like particle induced the reaction. One therefore has to conclude that short range correlations have to be implemented in the shell model to describe the nucleus probed by high-energy particles. Furthermore the data show that the parametrisation of the short range correlations by a delta-function reproduces only qualitatively the measurements.



ACKNOWLEDGEMENT

We wish to thank the directors of our institutions for the encouragement of this experiment.

We are obliged to the synchrotron group, the hall-service group, and all the technical groups at DESY for their excellent support of this experiment. The assistance of Ing. H. Sindt in constructing, testing, and carrying out the experiment is gratefully acknowledged.

This work was supported by the Bundesministerium für Forschung und Technologie.

REFERENCES

1. G. Jacob, T.A.J. Maris  
Nucl. Phys. 31, (1962) 139
2. U. Amaldi, G. Campos Venuti, G. Cortellessa, E. De Sanitis  
S. Frallani, R. Lombard and P. Salavadori  
Phys. Lett. 25B, (1967) 24
3. H. Hiramatsu, T. Kamae, H. Muramatsu, K. Nakamura  
Phys. Lett. 44B, (1973) 50
4. D. Zeller  
thesis Karlsruhe 1973 and  
DESY, Internal report F23-73/2
5. S. Galster, G. Hartwig, H. Klein, J. Moritz, K.H. Schmidt,  
W. Schmidt-Parzefall, H. Schopper and D. Wegener  
Nucl. Instr. Meth. 76, (1969) 337
6. S. Galster, G. Hartwig, H. Klein, J. Moritz, K.H. Schmidt,  
W. Schmidt-Parzefall, D. Wegener and J. Bleckwenn  
KFK-Bericht 963 (1969), Kernforschungszentrum Karlsruhe
7. C.D. Epp, T.A. Griffy  
Phys. Rev. C1, (1970) 1633
8. L.R.B. Elton, A. Swift  
Nucl. Phys. A94, (1967) 52
9. R. Jastrow  
Phys. Rev. 98, (1955) 1479
10. B. Blum  
thesis Erlangen 1972

11. V. Devanathan  
Ann. Phys. (N.Y.) 43, (1967) 741
12. L.W. Mo, Y.S. Tsai  
Rev. Mod. Phys. 41, (1969) 205
13. F.H. Heimlich  
thesis Freiburg 1973 and  
DESY, Internal report F23-73/1
14. W. Weise  
Phys. Lett. 38B, (1972) 301  
L.E. Wright, S.T. Tuan, M.G. Huber  
Lett. el Nuovo Cimento I, (1970) 253  
K. Chung, M. Danos, M.G. Huber  
Z.f.Phys. 240, (1970) 195

FIGURE CAPTIONS

Fig. 1 Angular distribution of the recoil proton compared to shell model calculations including short range nucleon-nucleon correlations with  $q_c = 300$  MeV/c.  $\theta_e$  = electron scattering angle,  $\theta_p$  = proton scattering angle.

Fig. 2 Momentum distribution of the bound state protons from  $^{12}\text{C}$  normalized in the maximum.

TABLE 1: Momentum distribution of bound state protons in  $^{12}\text{C}$

	$E_1 = 2.5 \text{ GeV}, \theta_e = 12^\circ$		$E_1 = 2.7 \text{ GeV}, \theta_e = 13.8^\circ$		$E_1 = 2.7 \text{ GeV}, \theta_e = 15^\circ$	
$p_2$ [fm $^{-1}$ ]	$ W(p) \cdot p ^2$	error [%]	$ W(p) \cdot p ^2$	error [%]	$ W(p) \cdot p ^2$	error [%]
0.04	0.021	12.1	0.025	13.4	0.030	9.1
0.12	0.075	3.4	0.078	3.2	0.075	2.6
0.20	0.184	2.4	0.187	2.2	0.191	1.9
0.28	0.383	1.8	0.383	1.8	0.378	1.6
0.36	0.559	1.7	0.557	1.6	0.552	1.5
0.44	0.759	1.5	0.763	1.6	0.722	1.5
0.52	0.938	1.4	0.897	1.5	0.869	1.5
0.60	0.998	1.4	0.989	1.5	0.973	1.5
0.68	1.000	1.5	1.000	1.6	1.000	1.6
0.76	0.985	1.7	0.991	1.7	0.999	1.8
0.84	0.951	2.1	0.950	1.9	0.941	1.9
0.92	0.883	2.6	0.881	2.1	0.860	2.0
1.00	0.806	3.7	0.723	2.7	0.697	2.4
1.08	0.761	4.9	0.684	4.0	0.584	3.1
1.16	0.631	7.1	0.609	6.3	0.506	4.2
1.24	0.525	9.1	0.498	8.4	0.416	5.7
1.32	0.457	12.5	0.457	9.8	0.341	7.8
1.40	0.409	15.8	0.363	13.4	0.278	11.6
1.48	0.346	20.6	0.306	19.5	0.275	16.5
1.56	0.296	28.9	0.282	25.6	0.273	23.8
1.64	0.274	39.6	0.261	34.8	0.244	36.9
1.72	0.268	56.9	0.255	57.4	0.277	51.0
1.80	0.242	81.7	0.263	82.3	0.309	70.9
1.88	0.200	112.0	0.248	137.0	0.266	104.0
1.96	0.185	142.0	0.209	152.0	0.226	166.0
2.04	0.171	173.0	0.184	199.0	0.181	240.0
2.12	0.076	304.0	0.103	321.0	0.142	417.0
2.20	0.011	951.0	0.057	910.0	0.078	801.0

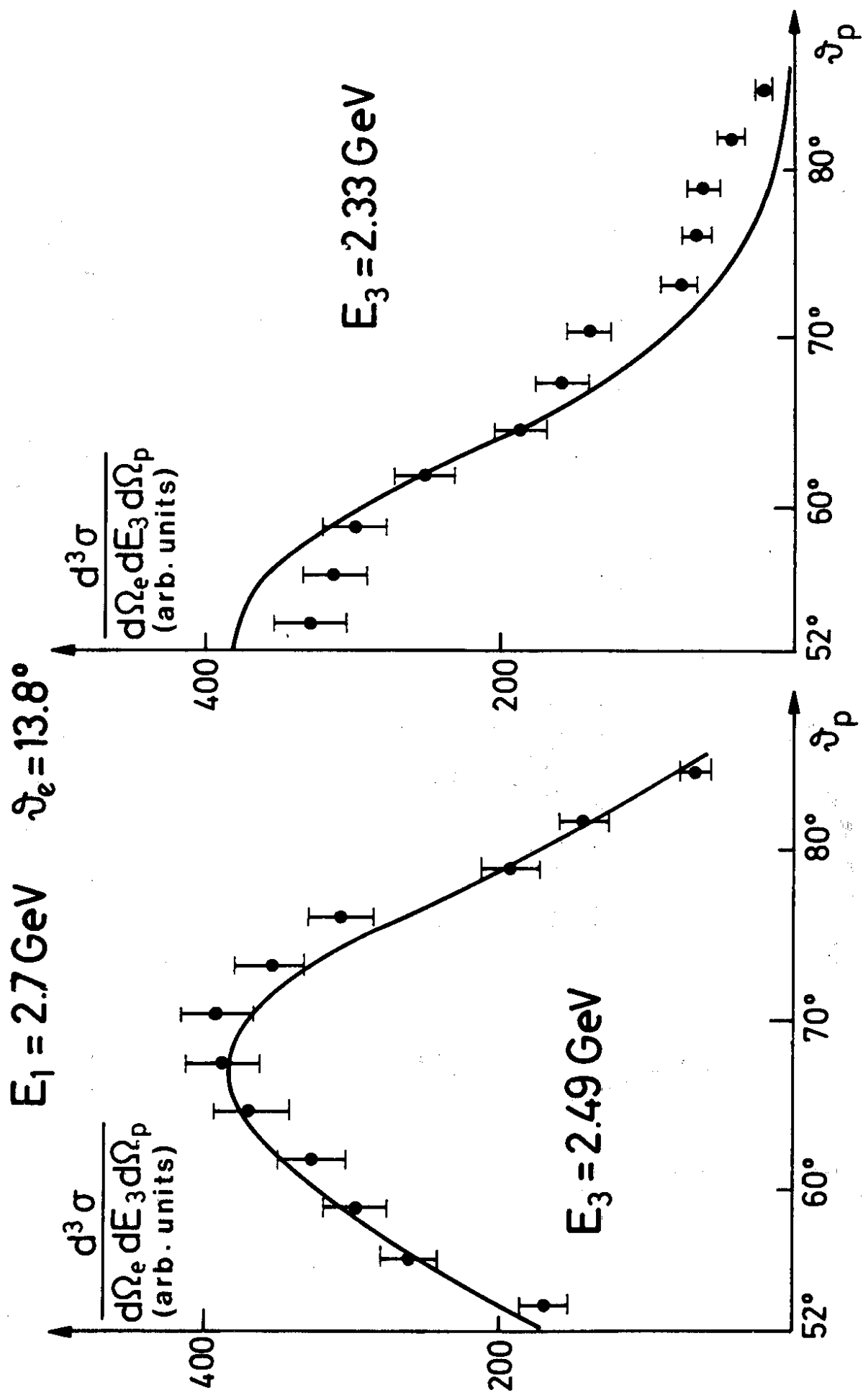


FIG.1

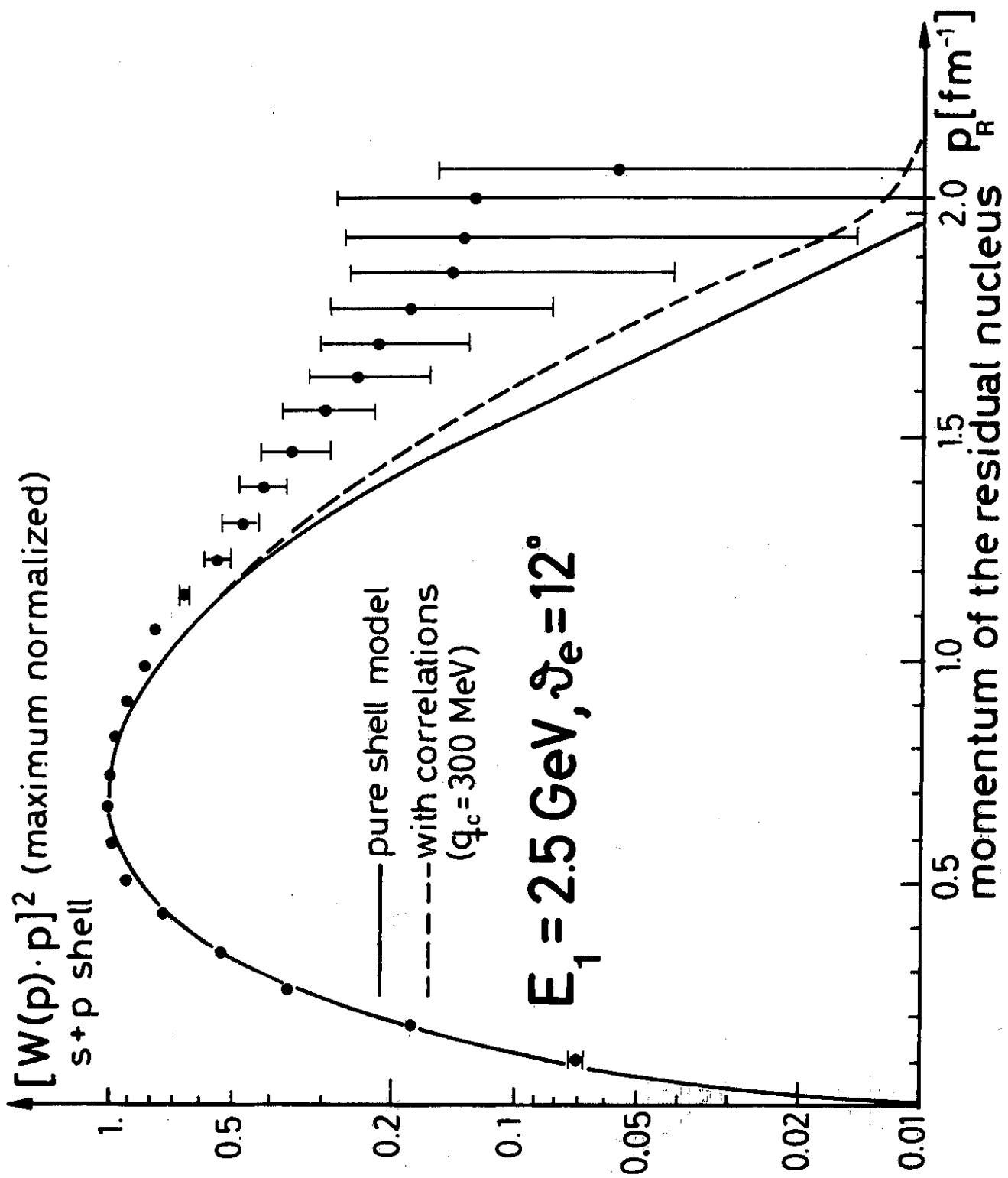


FIG.2